Dependence of the Second-order G'-band profile on the electronic structure of Single-wall nanotubes

A. G. Souza Filho,[a] A. Jorio[b], G. Dresselhaus[b], M. S. Dresselhaus[b], A. K. Swan,[c] M. S. Unlu,[c] B. B. Goldberg,[c], J. H. Hafner,[d] C. M. Lieber,[d] M. A. Pimenta[e], R. Saito[f]

[a] *Univ. Federal do Ceará, Fortaleza, CE 60455-900 Brazil;*
[b] *Massachusetts Institute of Technology, Cambridge, MA 02139-4307;*
[c] *Boston University, Boston, MA 0225;*
[d] *Harvard University, Cambridge, MA 02138;*
[e] *Univ. Federal de Minas Gerais, Belo Horizonte, MG 30123-970 Brazil;*
[f] *Univ. of Electro-Communications, Tokyo, 182-8585 Japan.*

ABSTRACT

We analyze the dependence of the second-order G'-band profile on their (n, m) indices by measuring the resonance Raman spectra of several semiconducting and metallic isolated tubes. We show that this profile is very sensitive to the electronic structure, thus making it possible to get structural (n, m) information and to probe the splitting of the van Hove singularities in the electronic density of states arising from the trigonal warping effect.

INTRODUCTION

Resonance Raman scattering (RRS) has been established as a powerful technique to investigate single-wall carbon nanotubes (SWNTs), providing valuable information about their electronic density of states (DOS)[1]. The recent observation of Raman spectra from just one SWNT has provided a new scenario in their study, whereby the Raman spectral properties has been successfully applied to determine the (n, m) indices.[2] Furthermore, single nanotube spectroscopy has allowed us to observe at the single nanotube level each feature appearing in the usual Raman spectrum for SWNT bundles. This possibility allows us to study the dependence of each feature on nanotube diameter d_t and chiral angle θ, or equivalently on the SWNT (n, m) indices.[3]

The Raman spectrum of SWNTs is relatively simple, where the main features are the radial breathing mode (RBM), the tangential G-band modes, the disorder-induced D-band, and the corresponding second-order G'-band.[1] Single nanotube spectroscopy has revealed that behind each spectral feature there are large amounts of new physical phenomena concerning their dependence on diameter and chirality. This work deals with the second order G'-band. Both the D-band and its G'-band overtone appear in the phonon spectra of sp^2 carbon-based materials and their frequencies are dependent on the laser excitation energy E_{laser} as a consequence of a double resonant process involving electron and phonon states close to the boundary of the Brillouin zone.[4, 5] The D-band is characteristic of disordered materials, while the G'-band is an intrinsic spectral feature of the graphite lattice.[4] Noteworthy is the fact that both the D-band and G'-band frequencies ω_D and $\omega_{DG'}$ are strongly dependent on the electronic structure of the nanotube and ω_D and $\omega_{DG'}$ can be used as a probe to obtain information on the electronic structure. This is the goal of the present work.

EXPERIMENT

The isolated SWNTs were grown using the chemical vapor deposition method (CVD) on a Si/SiO_2 substrate and the details of the process are reported elsewhere.[6] Raman spectra from each isolated SWNT were obtained by scanning the sample in steps of 0.5 μm under a controlled microscope stage. The spectral excitation was here provided by an Ar ion laser, using the 514.5 nm laser line (2.41 eV) and with a power density of $\sim$ 1 MW/cm^2. The scattered light was analyzed with a Renishaw spectrometer 1000B, equipped with a cooled charge coupled device (CCD) detector.

RESULTS AND DISCUSSION

The D-band and G′-band in SWNTs

Earlier studies in SWNTs bundles showed that the G'-band exhibits a dispersion behavior quite different from that for other sp^2 carbon materials.[7] An oscillatory behavior was observed[7] superimposed on a linear $\omega_{G'}$ vs. $E_{\rm laser}$ dependence, characteristic of graphite. This oscillatory behavior arises from the 1D electronic structure of the SWNTs. Studies at the single nanotube level have shown that both the D-band and G'-band frequencies ($\omega_{G'} \approx 2\omega_D$) show different values at the same laser excitation energy, thus exhibiting a dependence on (n, m) indices. This chirality dependence of ω_D is shown in Fig. 1(a), where ω_D data are plotted for 11 SWNTs with similar diameters vs. the chiral angle θ as determined by their (n, m) assignment, for which $E_{\rm laser}$ is resonant with E^S_{44}. The D-band and G'-band in graphite has its origin in a double resonance process, for which a large number of states with phonon wave vectors satisfying $q = 2k$ (where k is the electron wave vector) contribute to the D-band spectra. In the case of nanotubes, the quantized wave vectors k_{ii} play a fundamental role in determining the resonant process, as is clearly seen, when we plot the k_{ii} in terms of the chiral angle dependence of $\omega_D(\theta)$ as shown in Fig. 1. In Fig. 1(b) the open circles denote the predicted (n, m) indices that can be resonant and the stars over the open circles denote the SWNTs we actually observed in the Raman experiments. The good agreement between Figs. 1(a) and (b) shows that the $\omega_D(\theta)$dependence in SWNTs can be explained in terms of the relation between $|k_{ii}|$ for electrons and q for phonons to which electrons are strongly coupled by the double resonance process.[8] Through this agreement, we establish that, in the case of SWNTs, the double resonance is restricted to k_{ii} states corresponding to the van Hove singularities. It is interesting to note that the quantized k_{ii} vectors for the possible tubes for which E^S_{44} is resonant with $E_{\rm laser}$=2.41 eV are not random as a function of chirality, but $k_{ii}(\theta)$ indeed exhibits subband-like behavior. The similar pattern as a function of chirality for the k_{ii} and the observed $\omega_D(\theta)$ frequencies tell us that the (n, m) assignment is reliable, for otherwise $\omega_D(\theta)$ and k_{ii} would not be correlated with each other as they are. The importance of k_{ii} in the interpretation of the G'-band spectra is further discussed below.

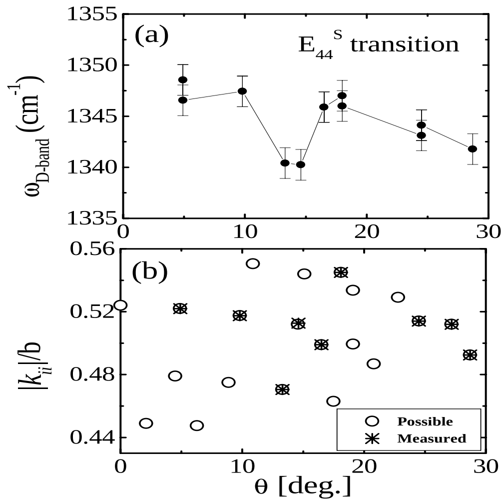

Figure 1: (a) Measured D-band frequencies as a function of chiral angle θ of SWNTs for which $E_{\rm laser}$ is in resonance with the E_{44}^{S} interband transitions. (b) The distance $|k_{ii}|$ to the K point for electrons in the 2D Brillouin zone of graphite, associated with the E_{ii} van Hove singularities, plotted vs. θ for the possible resonant tubes (open circles). The k_{ii} values for the observed tubes in (a) are plotted as stars over the open circles.

TWO PEAK EFFECTS IN THE G'-BAND

Semiconducting tubes

Figure2 (left panels) shows three G-band spectra for different isolated SWNTs with their respective (n,m) assignments implied by the RBM properties.[2] The G'-band in (a) and (b) are tubes for which $E_{\rm laser}$ is resonant with E_{44}^{S} and in (c) with E_{33}^{S}. The G'-band for most of the tubes show a single Lorentzian peak, as in (b) and (c). Some SWNTs show a "two peak effect" as in (a). The G'-band profile can be understood by analyzing the resonant process of $E_{\rm laser}$ with the singularities in the joint density of states (JDOS) shown in the right panels, keeping in mind that the quantized states k_{ii} determine the G' band frequencies. By examining the JDOS we see that for the (15,7) SWNT, $E_{\rm laser}$ (incident photon) is resonant with E_{44}^{S} and $E_{\rm laser} - E_{G'}$ (scattered photon) is resonant with E_{33}^{S}. It should be emphasized that this resonance occurs as two independent processes. Then, the double peaks observed for (15,7) arise from the resonance processes involving k_{44} (upper frequency component) and k_{33} (lower frequency component). Furthermore, one can use the G'-band dispersion measured in bundles (106 cm^{-1}/eV) to estimate the predicted splitting by multiplying 106$\times(E_{44}^{S} - E_{33}^{S})$ = 34 cm^{-1} for the (15,7) SWNT. The observed splitting in (a) is 35 cm^{-1}, in very good agreement with the prediction.

The G'-band profile in Fig. 2(b) and (c) has a single Lorentzian peak because only the incident photon is resonant. For the (17,7) tube [as identified below], the singularity E_{33} is too far from the energy of the scattered photon to allow the resonance to occur. The analysis of the G'-band profile can impose further restrictions to make the (n,m) assignment from the RBM analysis more reliable. For $\omega_{\rm RBM}$=148 cm^{-1}, there are two likely (n,m) candidates, namely, the (17,7) and (16,8) SWNTs. The (16,8) is eliminated from the assignment because the E_{33}^{S} energy would give rise to a strong resonance with the scattered photon, and two peaks in the G'-band would then be expected, so we conclude that the $\omega_{\rm RBM}$=148 cm^{-1} SWNT here corresponds to $(n,m) = (17,7)$. For tubes resonant

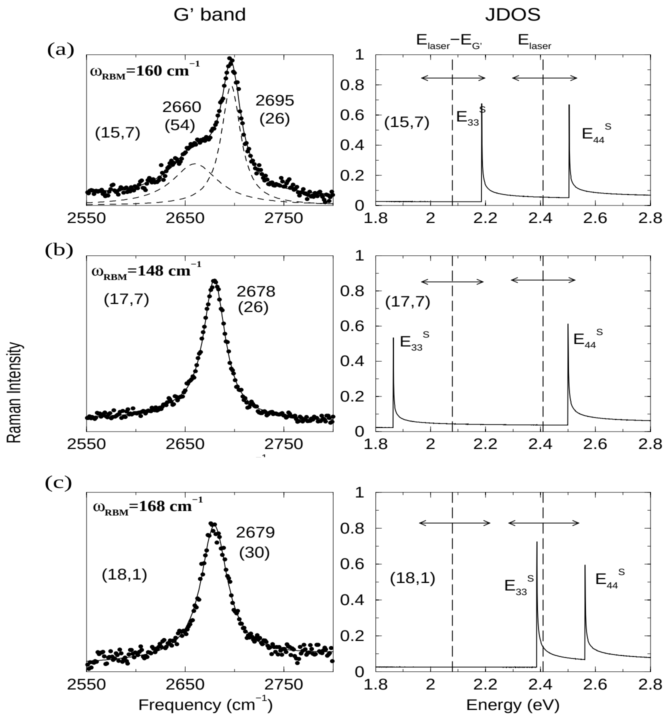

Figure 2: G'-band profile (left panels) and the JDOS (right panels) for the (15,7), (17,7), (18,1) SWNTs. The incident photon with $E_{\rm laser}$ = 2.41 eV is resonant with E_{44}^S for both the (15,7) and (17,7) SWNTs and with E_{33}^S for the (18,1) SWNT. The scattered photon at $E_{\rm laser} - E_{G'} \approx$2.08 eV is resonant with E_{33}^S for the (15,7) tube, but not for (17,7) and (18,1). Vertical dashed lines at 2.41 eV and 2.08 eV denote incident and scattered photons, respectively, and horizontal double arrows denote corresponding resonant windows. The numbers in parentheses denote linewidths. All frequencies and linewidths are in units of cm^{-1}.

with E_{44}^S, there are 8 (9) tubes predicted to exhibit a double peak (single peak), and we observed 4 (4) of them. No exceptions to the predictions of double (single) peaks were found.

Interesting is the case of the (18,1) SWNT, for which $E_{\rm laser}$ is resonant with E_{33}^S. Actually, all the tubes resonant with E_{33}^S are predicted to exhibit only one peak because the E_{22}^S interband transition is far from the scattered photon energy for all possible (n,m). For tubes resonant with E_{33}^S, among all 10 tubes predicted to exhibit a single peak, we observed 5 of them.

Metallic tubes

The metallic tubes we studied in this experiment were all measured for the resonance of $E_{\rm laser}$=2.41 eV with the E_{22}^M singularities. Due to the trigonal warping effect, each van Hove singularity for a metallic nanotube is predicted to exhibit a splitting, depending on its chirality. The magnitude of this splitting varies from zero for armchair nanotubes (n,n) [n integer] to a maximum splitting for metallic zigzag nanotubes $(n,0)$ [$n=3p$, p integer].[9] Using the analysis presented above, a double peak effect in the G'-band profile is expected also for trigonal warping. First, all the armchair nanotubes (n,n) are predicted to exhibit a G'-band profile composed of a single Lorentzian line, since there is no trigonal-warping-based splitting for armchair tubes and the energy difference between subband resonances E_{22}^M and E_{11}^M is very large. One tube, (15,15) is predicted to be resonant with $E_{\rm laser}$=2.41 eV and we did indeed observe this particular nanotube, whereby the G'-band has a single Lorentzian lineshape

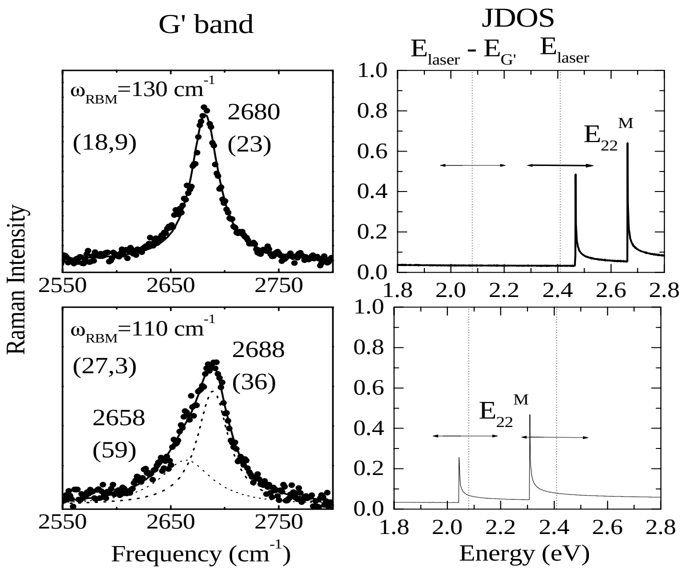

Figure 3: Same as in the Fig. 2, except for the data to (18,9) and (27,3) SWNTs and the singularities in JDOS is here E_{22}^{M} [10].

centered at 2680 cm^{-1} and 31 cm^{-1} in linewidth. Figure 3 shows the G'-band profile for two metallic SWNTs tentatively assigned as (18,9) (upper panel) and (27,3) (lower panel). The (18,9) has a G'-band with a single Lorentzian line shape in agreement with its JDOS, for which the only resonance is for the incident photon with the lower E_{22}^{M} component. This is not the case for the (27,3) tube where the same two peak effect in the G'-band profile is observed, in agreement with the calculated JDOS for this tube.

Among the 17 metallic SWNTs predicted to be observed in resonance with 2.41 eV, we did observe 8 of them consisting of 3 metal-1 and 5 metal-2 SWNTs.[10] We found that the splitting observed in the G'-band is linearly correlated to the splitting ΔE_{22}^{M} and a fit to the experimental data leads to $\Delta\omega_{G'} = (108 \pm 6)\Delta E_{22}^{M}$. This slope, which is in a very good agreement with the observed G'-band dispersion in SWNT bundles (106 cm^{-1}/eV), provides a direct measurement of the G'-band dispersion using measurements with only one laser line.

Finally, the agreement between the predictions and observations allows us to conclude that the origin of both the D-band and G'-band in semiconducting and metallic (metal-1 and metal-2) SWNTs is due to the same basic mechanism that stems from resonance with the quantized k_{ii} states. Our experiments do not confirm the prediction made by Maltzusch et al.[11], where only metal-1 SWNTs are predicted to exhibit the G'-band feature. Our experimental results are, however, consistent with the predictions by Kürti et al.[12] who found the calculated D-band intensity to have a maximum when a van Hove singularity is in resonance with either the incident or scattered photon.

CONCLUSIONS

In summary, we have studied two-peak effects in the second-order G'-band in individual single-wall carbon nanotubes, including both semiconducting and metallic SWNTs. Although some of the G'-band profiles show single Lorentzian

peaks, some of the tubes show a two-peak structure. In semiconducting tubes, the double peak is identified with the superposition of two independent resonant processes, whereby one singularity (E_{44}^S) is resonant with the incident photon (E_{44}^S), and the other(E_{33}^S) involves the scattered photon. In the case of metallic tubes, a similar two peak effect is observed, but now the resonant processes occurs with the two components of the same singularity E_{22}^M, arising from the trigonal warping effect. By combining the role of the confined electronic states k_{ii} in determining the phonon frequencies $\omega_{G'}$, we show that the G'-band profile gives confirmatory structural information about the (n, m) assignment, provides a method to probe the electronic trigonal warping effect in metallic tubes quantitatively, and yields the G'-band dispersion of 108 ± 6 cm^{-1}/eV using only one laser line.

ACKNOWLEDGMENTS

A.G.S.F. and A.J. acknowledge financial support from the Brazilian agencies CAPES and CNPq, respectively. MIT authors acknowledge support under NSF Grants DMR 01-16042, INT 98-15744. R.S. acknowledges Grant-in-Aid (No. 13440091) from Ministry of Education, Japan. We acknowledge the NSF/CNPq joint collaboration program (NSF INT 00-00408 and CNPq Grant No. 910120/99-4)

REFERENCES

[1] M. S. Dresselhaus and P. C. Eklund, Advances in Physics **49**, 705 (2000).

[2] A. Jorio, R. Saito, J. H. Hafner, C. M. Lieber, M. Hunter, T. McClure, G. Dresselhaus, and M. S. Dresselhaus, Phys. Rev. Lett. **86**, 1118 (2001).

[3] For a review on single nanotube spectroscopy see [M. S. Dresselhaus, G. Dresselhaus, A. Jorio, A. G. Souza Filho, and R. Saito, Carbon (2002), submitted]

[4] A. V. Baranov, A. N. Bekhterev, Y. S. Bobovich, and V. I. Petrov, Opt. Spectrosc. USSR **62**, 612 (1987).

[5] M. J. Matthews, M. A. Pimenta, G. Dresselhaus, M. S. Dresselhaus, and M. Endo, Phys. Rev. B **59**, 6585(R) (1999).

[6] J. H. Hafner, C. L. Cheung, T. H. Oosterkamp, and C. M. Lieber, J. Phys. Chem. B **105**, 743 (2001).

[7] M. A. Pimenta et al., Brazilian J. Phys. **30**, 423 (2000).

[8] C. Thomsen and S. Reich, Phys. Rev. Lett. **85**, 5214 (2000).

[9] R. Saito, G. Dresselhaus, and M. S. Dresselhaus, Phys. Rev. B **61**, 2981 (2000).

[10] R. Saito, G. Dresselhaus, and M. S. Dresselhaus, *Physical Properties of Carbon Nanotubes* (Imperial College Press, London, 1998).

[11] J. Maultzsch, S. Reich, and C. Thomsen, Phys. Rev. B **63**, 121407(R) (2001).

[12] J. Kürti, V. Zölyomi, A. Grüeneis, and H. Kuzmany, Phys. Rev. B (2001), submitted.